HHS Public Access

Author manuscript

Int J Biochem Cell Biol. Author manuscript; available in PMC 2017 February 01.

Published in final edited form as:

Int J Biochem Cell Biol. 2016 February ; 71: 72–80. doi:10.1016/j.biocel.2015.12.010.

Absence of AMPK 2 Accelerates Cellular Senescence via P16 Induction in Mouse Embryonic Fibroblasts

Ye Ding[§], **Jie Chen**[§], **Imoh Sunday Okon**, **Ming-Hui Zou**, and **Ping Song**[*]

Center for Molecular and Translational Medicine, Georgia State University, Atlanta, Georgia, 30303

Abstract

Emerging evidence suggests that activation of adenosine monophosphate-activated protein kinase (AMPK), an energy gauge and redox sensor, delays aging process. However, the molecular mechanisms by which AMPKα isoform regulates cellular senescence remain largely unknown. The aim of this study was to determine if AMPKα deletion contributes to the accelerated cell senescence by inducing $p16^{INK4A}$ (p16) expression thereby arresting cell cycle. The markers of cellular senescence, cell cycle proteins, and reactive oxygen species (ROS) were monitored in cultured mouse embryonic fibroblasts (MEFs) isolated from wild type (WT, C57BL/6J), AMPKα1, or AMPKα2 homozygous deficient ($AMPK\alpha1^{-/-}$, $AMPK\alpha2^{-/-}$) mice by Western blot and cellular immunofluorescence staining, as well as immunohistochemistry (IHC) in skin tissue of young and aged mice. Deletion of AMPKα2, the minor isoform of AMPKα, but not AMPKα1 in high-passaged MEFs led to spontaneous cell senescence demonstrated by accumulation of senescence-associated-β-galactosidase (SA-β-gal) staining and foci formation of heterochromatin protein 1 homolog gamma (HP1γ). It was shown here that AMPKα2 deletion upregulates cyclin-dependent kinase (CDK) inhibitor, p16, which arrests cell cycle. Furthermore, AMPKα2 null cells exhibited elevated ROS production. Interestingly, knockdown of HMG box-containing protein 1 (HBP1) partially blocked the cellular senescence of AMPKα2-deleted MEFs via the reduction of p16. Finally, dermal cells senescence, including fibroblasts senescence evidenced by the staining of p16, HBP1, and Ki-67, in the skin of aged $AMPK\alpha2^{-/-}$ mice was enhanced when compared with that in wild type mice. Taken together, our results suggest that AMPKα2 isoform plays a fundamental role in anti-oxidant stress and anti-senescence.

Keywords

AMPKα2; HBP1; p16; reactive oxygen species; cellular senescence

[*]To whom correspondence should be addressed: Ping Song, Ph.D., Center for Molecular and Translational Medicine, Georgia State University, 161 Jesse Hill Jr Dr SE, Atlanta, GA, 30303, USA, Tel: (404) 413-6636, Fax: (404) 413-3580, psong@gsu.edu.
[§]These authors contributed equally to this work.

1. Introduction

Cellular senescence, an irreversible cell-cycle arrest, plays pivotal roles in physiology, such as normal embryonic development (Munoz-Espin and Serrano, 2014), as well as pathological processes, including aging and age-related disorders (Baker et al., 2011; Lopez-Otin et al., 2013; van Deursen, 2014), cardiovascular disease (Fyhrquist et al., 2013; Kovacic et al., 2011), and type II diabetes (Testa and Ceriello, 2007). Cell senescence is triggered and driven by many factors including oxidative stress, DNA damage, telomere shortening, chronic inflammation, and mitogenic signals (Fyhrquist et al., 2013). The molecular mechanisms underlying cellular senescence are complicated and still obscure. The most common mediators of senescence are $p16^{INK4A}$ (p16), $p14^{ARF}$, p53 (Rufini et al., 2013), p21, p15, p27, and hypophosphorylated retinoblastoma (Rb). Among them, the cyclin-dependent kinase (CDK) inhibitor, p16 is a key modulator of cell senescence (Sorrentino et al., 2014), and plays an important role in the initiation and maintenance of cellular senescence (Rayess et al., 2012). Thus, p16 is also used as a biomarker of senescent cells and aging process (Burd et al., 2013; Janzen et al., 2006; Krishnamurthy et al., 2004; Sorrentino et al., 2014). Regulation of p16 is complex and involves epigenetic control (Zheng et al., 2013) and multiple transcription factors, including polycomb protein Bmi-1 (Meng et al., 2010), Ets1 (Ohtani et al., 2001), and HMG box-containing protein 1 (HBP1) (Li et al., 2010; Wang et al., 2012b).

Adenosine monophosphate-activated protein kinase (AMPK) is evolutionarily conserved and exerts its essential functions in metabolism (Ruderman et al., 2013), redox response and regulation (Song and Zou, 2012), as well as cell growth (Song et al., 2011). Mammalian AMPK is a serine/threonine protein kinase consisting of a catalytic α subunit and regulatory β and γ subunits, each of which has at least two isoforms (Hardie, 2007). Recently, several reports have indicated that AMPK plays an important role in aging process and longevity of lower organisms (Salminen and Kaarniranta, 2012). AAK-2 (AMPKα in *Caenorhabditiselegans*) is required for lifespan extension by inhibition of insulin/insulin-like growth factor 1 (IGF-1) signaling (Apfeld et al., 2004; Chen et al., 2013). AMPKα2 activation by 5'-aminoimidazole-4-carboxamide-1-β-D-ribofuranoside (AICAR) and exercise is impaired in skeletal muscle of aged rats (28-month-old) (Reznick et al., 2007). In addition, transgenic expression of AMPK in adult fat body or muscle can extend life span in *Drosophila*. Conversely, AMPK knockdown by RNAi reduces longevity of flies (Stenesen et al., 2013). Furthermore, the acetylation of yeast Sip2, a regulatory β subunit of Snf1 complex (yeast AMPK) decreases as yeast cells age. Mechanistically, Sip2 acetylation enhances its association with Snf1, the catalytic subunit of Snf1 complex, and inhibits Snf1 activity, thus reducing the phosphorylation of a downstream target, Sch9 (homolog of Akt/S6K), and ultimately resulting in slower growth but extended life span (Lu et al., 2011). On the other hand, the senescence of in vitro human fibroblast induced by low energy stress is accompanied by increased AMPK activity (Wang et al., 2003). However, whether mammalian AMPK is causally implicated in cellular senescence and whether its depletion is detrimental remain elusive. What is the exact role of AMPKα isoform in cell senescence? Is AMPKα deletion associated with skin aging in mice *in vivo*? To address these fundamental questions, we investigated cellular senescence and the underlying mechanism in $AMPK\alpha^{-/-}$

mouse embryo fibroblasts (MEFs). We demonstrate here, for the first time, that AMPKα2$^{-/-}$ MEFs exhibit accelerated cellular senescence due to p16 induction controlled by transcription factor HBP1 and consequent cell cycle arrest. These findings establish a new role for AMPKα2 in anti-oxidant events and aging, providing novel insights into the mechanism of tumor suppression or wound healing mediated by AMPK.

2. Materials and methods

2.1. Materials and reagents

The following antibodies were obtained from Cell Signaling Technology (Beverly, MA): rabbit anti-CDK2 (2546), mouse anti-Cyclin B1 (4135), and rabbit anti-PCNA (13110). The following antibodies were purchased from Santa Cruz Biotechnology (Santa Cruz, CA): mouse anti-p16 (sc-74400), mouse anti-GAPDH (sc-32233), mouse anti-β-actin (sc-47778), mouse anti-E2F-1 (sc-251), rabbit anti-HBP1 (sc-25390), mouse anti-Bmi-1(sc-13519), and mouse anti-Ets-1 (sc-55581). Rabbit anti-SOD1 (ab16831), rabbit anti-SOD2 (ab13533), and rabbit anti-Ki-67 (ab15580) were purchased from Abcam (Cambridge, MA). Mouse anti-HP1γ antibody (05-690) and rabbit anti-H3K9me3 (07-442) antibody were purchased from EMD Millipore (Billerica, MA). Other chemicals and organic solvents of the highest available grade were obtained from Sigma-Aldrich. AMPKα1$^{-/-}$ and AMPKα2$^{-/-}$ mice were described elsewhere (Jorgensen et al., 2004; Viollet et al., 2003). Mice were handled in accordance with study protocols approved by the Institutional Animal Care and Use Committee of Georgia State University (Atlanta, GA).

2.2. Cell culture, transfection, and infection

Mouse embryonic fibroblasts (MEFs) were isolated from WT, AMPKα1$^{-/-}$, and AMPKα2$^{-/-}$ mouse embryos at 13.5-days post-coitus and cells were passaged with the 3T3 protocol as described previously (Todaro and Green, 1963; Wang et al., 2012a). Briefly, 13.5-day mouse embryo was decapitated, thoroughly minced, and trypsinized. The dissociated cells were re-suspended and passaged consecutively according to the 3T3 protocol (3×10^5 cells were seeded per 60-mm dish every 3 days) until the growth rates in culture stabilized. Cells were then cultured for an additional 20 passages (to about passage 40) and were considered high-passaged and used for experiments at that point. MEFs were maintained in Dulbecco's modified Eagle's medium (Invitrogen, Carlsbad, CA) supplemented with 10% FBS, L-Glutamine (2 mM) (Lonza, Walkersville, MD), penicillin (100 U/ml), and streptomycin (100 μg/ml) (Life Technologies, Grand Island, NY). Mouse HBP1 siRNA (sc-35533) and siRNA duplex controls to be used are from Santa Cruz Biotechnology. Transfection of the siRNA will be performed with Lipofectamine® RNAiMAX Transfection Reagent (ThermoFisher Scientific) in Opti-MEM I serum-reduced medium (GIBCO) according to the methods described previously (Song et al., 2009). MEFs were transiently infected with GFP, SOD1, SOD2, or catalase (MOI=50) for 48 h as previously reported (Xu et al., 2015).

2.3. Indirect immunofluorescence and microscopy

Cells were grown on poly-L-lysine-coated glass coverslips. Cell were fixed in 4% paraformaldehyde, permeabilized in 0.1% TritonX-100 and blocked with image-IT Fix or

BSA (Invitrogen). Primary antibodies used were: mouse anti-HP1γ (1:100 v/v) or rabbit anti-H3K9me3 (1:100 v/v). DNA was stained with anti-fade reagent with 4',6-diamidino-2-phenylindole (DAPI) (Invitrogen, Carlsbad, CA). For indirect immunofluorescence, Alexa Fluor® 488 and 555 were used for detection of the protein. Confocal microscopy was performed using a Zeiss 710 confocal microscope (Oberkochen, Germany), with a 63× oil immersion lens. Image editing was performed in Adobe Systems Incorporated, San Jose, CA.

2.4. Immunohistochemical staining

Skins were collected from 5-month-old and 24-month-old wild type and AMPKα2 knockout mice and fixed in 4% paraformaldehyde. The tissue samples were dehydrated and embedded in paraffin wax. Serial paraffin sections (4 μm) were obtained and kept at 37℃ for more than 12 h. The sections were immersed in three consecutive washings in xylol for 5 min to remove paraffin, and then hydrated with five consecutive washings with alcohol in descending order 100, 100, 90, 80, 70% and deionized water respectively. The slides were immersed in citrate buffer solution (0.01 mol/L, pH 6.0) and heated at 100℃ for 30 min, naturally cooled down and then immersed in 3% aqueous hydrogen peroxide for endogenous peroxidase ablation at room temperature for 20 min. The following steps were executed in a moist chamber. The sections were washed in PBS, quenched with blocking buffer (BioGenex, Fremont, CA). Sections were sequentially treated with primary antibody, secondary antibody (Dako, Carpinteria, CA) and DAB substrate (Dako, Carpinteria, CA). Finally, the tissue sections were counterstained with hematoxylin, dehydrated, cleared and mounted with neutral gums. In parallel, tissue specimens in which the primary antibody was replaced by PBS served as negative control.

2.5. RNA extraction, cDNA synthesis, and real-time PCR

Total mRNA was isolated and purified using the RNeasy mini kit from Qiagen (Valencia, CA) according to the manufacturer's instructions. cDNA was synthesized from isolated mRNA using the iScript cDNA synthesis kit (Bio-Rad Laboratories, Hercules, CA), as described previously (Song et al., 2011) and by the manufacturer's instructions. Real-time PCR was performed on a ABI PRISM 7700 sequence detection system (Applied Biosystems) with SYBR green PCR master mix (Applied Biosystems) and 1 μl of first-strand cDNA as template with specific primers for *p16* (5′ −TACCCCGATTCAGGTGATGATG−3′, 5′−TAGCTCTGCTCTTGGGATTGG−3′) . The levels of gene expression were determined relative to that of *β-actin* (5′ −TGGGCCGCTCTAGGCACCA−3′, 5′− ACCGGAATCCCAAGTCCCC−3′).

2.6. Senescence-associated β-galactosidase (SA-β-gal) staining

SA-β-gal staining was performed as previously described (Debacq-Chainiaux et al., 2009). Briefly, MEFs growing on 6-well plates were washed twice with PBS, fixed with 4% paraformaldehyde for 5 min at room temperature. The cells were then washed with PBS and incubated with fresh SA-β-gal staining solution (Cell Signaling Technology) at 37°C for 16–18 h to visualize SA-β-gal staining under an Olympus (Tokyo, Japan) microscope.

2.7. Protein extraction and immunoblotting

Whole cell extracts were collected using cell lysis buffer (9803) from Cell Signaling Technology with protease and phosphatase inhibitor cocktails I and II (Cat. # BP-479 and BP-480, Boston BioProducts, MA). Protein samples (30–50 μg) were separated by SDS-PAGE, transferred onto nitrocellulose membranes, and probed with different antibodies as previously described (Song et al., 2007; Song et al., 2009). Following incubation with the appropriate horseradish peroxidase-linked secondary antibodies (Cell Signaling Technology), signal was visualized with an enhanced chemiluminescence detection system (GE Healthcare) and quantified by densitometry. Equal loading of protein was verified by immunoblotting with anti-β-actin or -GAPDH antibody.

2.8. Statistical analysis

Unless otherwise stated, data were presented as mean ± S.D. Differences between multiple means were evaluated by two-tailed Student's *t* test or analysis of variance with post hoc Bonferroni corrections. A p value < 0.05 was considered statistically significant.

3. Results

3.1. AMPKα2 deletion enhances cellular senescence in MEFs

First, we characterized cell growth profiles of AMPKα1$^{-/-}$ and AMPKα2$^{-/-}$ MEFs along with control wild type (WT) cells by live cell counting. As shown in Fig. 1A, the growth rate of AMPKα2$^{-/-}$ MEFs was pretty slower, while AMPKα1$^{-/-}$ MEFs was significantly faster than WT MEFs, which is consistent with our previous result (Xu et al., 2015). Furthermore, the levels of cell cycle-associated proteins, including cyclin-dependent kinase 2 (CDK2), cyclin B1, and proliferating cell nuclear antigen (PCNA) in AMPKα1$^{-/-}$ MEFs were significantly higher than that in WT MEFs, while AMPKα2$^{-/-}$ MEFs had dramatically lower levels of these proteins when compared with WT MEFs (Fig. 1B). These data suggest that AMPKα2$^{-/-}$ MEFs display accelerated senescence due to defective proliferation. To test this hypothesis, an assay with senescence-associated-β-galactosidase (SA-β gal) activity, a biomarker of senescent cells (Debacq-Chainiaux et al., 2009), was applied with these MEFs. As depicted in Fig. 1C and 1D, much more AMPKα2$^{-/-}$ MEFs exhibited positive SA-β-gal staining when compared with either AMPKα1$^{-/-}$ MEFs or WT MEFs.

To confirm our observations of increased cell senescence in AMPKα2$^{-/-}$ MEFs, we examined trimethylated histone H3 on lysine 9 (H3K9me3), a critical feature of senescent cells (Braig et al., 2005), as well as heterochromatin protein 1 homolog gamma (HP1γ) foci formation, which is senescence-associated (Ha et al., 2008). Consistently, HP1γ foci formation was significantly increased in AMPKα2$^{-/-}$ MEFs, but not in either WT or AMPKα1$^{-/-}$ MEFs (Fig. 1E and 1F). Increased H3K9me3 staining was observed in both AMPKα1$^{-/-}$ and AMPKα2$^{-/-}$ MEFs with less extent (Fig. 1G). The discrepancy of HP1γ staining in AMPKα1$^{-/-}$ and AMPKα2$^{-/-}$ cells suggests that HP1γ rather than H3K9me3 is probably a more specific marker for the *de novo* senescence induction.

3.2. p16 protein is transcriptionally upregulated in AMPKα2$^{-/-}$ MEFs

Because p16 is the major negative regulator for cell cycle by Rb/E2F-1 pathway (Jung et al., 2007), we examined its profile in MEFs with different AMPK genetic background. As expected, p16 protein was dramatically elevated in AMPKα2$^{-/-}$ MEFs when compared with WT and AMPKα1$^{-/-}$ MEFs (Fig. 2A). However, E2F-1 protein, an important modulator in cell-cycle progression (O'Donnell et al., 2005), was markedly decreased in AMPKα2$^{-/-}$ MEFs (Fig. 2B). Furthermore, 26S proteasome inhibitor MG132 treatment did not further increase p16 protein levels (Fig. 2C), which imply that p16 upregulation in AMPKα2$^{-/-}$ MEFs does not attribute to a change in p16 protein stability. Importantly, qRT-PCR assay demonstrated that *p16* mRNA level was profoundly elevated in AMPKα2$^{-/-}$ MEFs when compared with WT MEFs (Fig. 2D).

3.3. HBP1 is responsible for the p16 induction in AMPKα2$^{-/-}$ MEFs

Because we have observed that p16 was transcriptionally upregulated in AMPKα2$^{-/-}$ MEFs, we further explored the potential transcriptional regulatory mechanisms that might be related to p16 expression. We subsequently analyzed three transcription factors that were shown to be essential direct regulators of p16 expression in several reports (Li et al., 2010; Meng et al., 2010; Wang et al., 2012b). Among the three transcription factors including HBP1, Ets-1, and Bmi-1, only HBP1 was significantly increased in AMPKα2$^{-/-}$ MEFs (Fig. 3A). There was no difference with either Ets-1 or Bmi-1 protein levels between WT and AMPKα2$^{-/-}$ MEFs (Fig. 3B). Since Bmi-1 was reported to negatively control p16 expression, here Bmi-1 was unlikely to contribute to the p16 elevation in AMPKα2$^{-/-}$ MEFs. These data suggest that HBP1 may function as a transcriptional factor for p16 induction in AMPKα2$^{-/-}$ MEFs. We further employed siRNA to knockdown HBP1 in order to validate the function of HBP1 in p16 regulation. As depicted in Fig. 3C, HBP1 depletion by siRNA significantly downregulated p16 protein level that was elevated in AMPKα2$^{-/-}$ MEFs. Furthermore, HBP1 siRNA dramatically decreased *p16* mRNA level in AMPKα2$^{-/-}$ MEFs when compared with control siRNA (Fig. 3D).

3.4. Increased ROS and its regulation on p16 in AMPKα2$^{-/-}$ MEFs

Given AMPK's function in defense against ROS (Song and Zou, 2012), we speculated that the induction of p16 may be mainly due to the accumulated ROS in MEFs. To test our hypothesis, we applied dihydroethidium (DHE) assay to detect the cellular level of ROS in MEFs, and observed a dramatic increase of superoxide anion ($O_2^{\cdot -}$) production in AMPKα2$^{-/-}$ MEFs (Fig. 4A).

It is known that ROS can induce premature senescence. To validate these results, we administered antioxidants 4-hydroxy-TEMPO (Tempol) and Mito-TEMPO to decrease the mitochondria-derived oxidative damage in the cells. The p16 level decreased dramatically in AMPKα2$^{-/-}$ MEFs after Tempol and Mito-TEMPO treatment, peaking at 24 hours post-treatment (Fig. 4B). The MEFs were also infected with superoxide dismutases (SOD) SOD1 and SOD2 as well as catalase, and p16 reduction was evident in AMPKα2$^{-/-}$ MEFs in response to either SOD2 or catalase overexpression (Fig. 4C). The result was similar to the Mito-TEMPO treatments (Fig. 4B). Furthermore, Mito-TEMPO significantly inhibited the senescence of AMPKα2$^{-/-}$ MEFs (Fig. 4D and 4E). Taken together, mitochondria-derived

ROS appears to be the major trigger for the activation of p16 expression, hence senescence induction in AMPKα2$^{-/-}$ MEFs.

3.5. HBP1 is responsible for cellular senescence in AMPKα2$^{-/-}$ MEFs

Since HBP1 controls p16 expression (Fig. 3), and p16 regulates cell senescence (Sorrentino et al., 2014), we validated whether HBP1 modulates cellular senescence in AMPKα2$^{-/-}$ MEFs. Intriguingly, HBP1 depletion by siRNA (Fig. 5C) significantly impeded cellular senescence in AMPKα2$^{-/-}$ MEFs (Fig. 5 A and 5B), which is consistent with HBP1 function in Ras-induced premature senescence (Li et al., 2010).

3.6. Enhanced cellular senescence in skin of AMPKα2$^{-/-}$ mice

Since AMPKα2 deletion accelerates MEFs senescence *in vitro*, we subsequently investigated whether AMPKα2 deletion affect cellular senescence in derma fibroblasts and skin aging. As depicted in Fig. 6*A*, the staining of Ki-67, extensively used as a proliferation marker (Inwald et al., 2013), in 24-month-old wild type (WT) mice was obviously weaker than that in young (5-month-old) WT mice (Fig. 6E). However, the staining of p16 (Fig. 6 C) in old WT mice, which highly reflects biological aging in human skin (Waaijer et al., 2012), was stronger than that in young WT mice (Fig. 6G). These data indicated that Ki-67 and p16 are tightly associated with cellular senescence and skin aging. For 5-month-old mice, the staining of Ki-67 in AMPKα2$^{-/-}$ mice was weaker than that in WT mice (Fig. 6A and 6E). Whereas, the staining of both HBP1 (Fig. 6B) and p16 (Fig. 6C) in AMPKα2$^{-/-}$ mice was stronger than that in WT mice (Fig. 6F and 6G). Intriguingly, for aged mice, the Ki-67 staining in AMPKα2$^{-/-}$ mice was much weaker than that in WT mice (Fig. 6 A and 6E). Moreover, the staining of both HBP1 (Fig. 6B) and p16 (Fig. 6C) in derma fibroblast (Fig. 6D) of aged AMPKα2$^{-/-}$ mice was very stronger than that in aged WT mice (Fig.6F and 6G). These results suggest that AMPKα2 deletion promotes cellular senescence and skin aging process, implying that AMPKα2 may be an important regulator of skin aging *in vivo*.

4. Discussion

In the current study, we have demonstrated that deletion of AMPKα2, but not AMPKα1 accelerates cellular senescence and cell cycle arrest in MEFs. The mechanism underlying this process is partly due to p16 upregulation (Fig. 7). Elevated p16 expression in AMPKα2$^{-/-}$ MEFs is due to the increased oxidative stress (Fig. 4B and 4C) and upregulated HBP1 (Fig. 3A and 3C). HBP1 knockdown blunts cell senescence (Fig. 5A and 5B). The absence of AMPKα2 causes accelerated skin aging. These results suggest that AMPKα2 is a pivotal regulator of anti-senescence, even anti-aging.

AMPK activation is reported to extend the lifespan of lower organisms, including *Caenorhabditis elegans* (Chen et al., 2013), Drosophila (Stenesen et al., 2013), and yeast (Jiao et al., 2015). However, the role of AMPK in mammalian cellular senescence and aging process is controversial. On the one hand, it is reported that activation of AMPK pathway promotes senescence in hepatoma cells exposed to low concentration of metformin in a p53-dependent profile (Yi et al., 2013). LKB1-dependent AMPK activation by adriamycin

promotes vascular smooth muscle cell senescence (Sung et al., 2011). AMPK drives the senescence of human T cells via p38 activation triggered by recruitment of p38 to scaffold protein TAB1 (Lanna et al., 2014). On the other hand, AMPK activation is involved in macrophage migration inhibitory factor (MIF)-mediated anti-senescence in mesenchymal stem cells (Xia et al., 2015). AMPK blocks hydrogen peroxide (H_2O_2)-induced premature senescence in auditory cells (Tsuchihashi et al., 2015). AMPK-FOXO3 pathway is involved in resveratrol-mediated anti-senescence induced by oxidative stress, H_2O_2 in cultured primary human keratinocytes (Ido et al., 2015). This discrepancy may be due to the different AMPKα isoform. Overexpression of constitutively active AMPKα1 isoform enhances senescence of human fibroblast, however, dominant-negative isoform of AMPKα1 blocks the fibroblast senescence (Wang et al., 2003), which may associate with the enhanced cellular proliferation (Xu et al., 2015). In addition, knock-down of liver kinase B1 (LKB1)/AMPK signal accelerates G1/S transition via p53/p16 pathway in human embryonic kidney 293T cells and human umbilical vein endothelial cells (Liang et al., 2010). Here we have, for the first time, identified that AMPKα2, but not AMPKα1 may mediate anti-senescence by employing embryonic fibroblast of AMPKα knockout mice as a cell model system.

Cellular senescence can be promoted by multiple factors, such as DNA damage, stress, and oncogene. Among them, oxidative stress plays an important role in initiation of cell senescence. AMPKα2 deletion increases superoxide production in endothelial cells via upregulation of NAD(P)H oxidase subunit expression, including $gp91^{phox}$, $p47^{phox}$, $p67^{phox}$, and NOX4 (Wang et al., 2010). Here, it was demonstrated that AMPKα2 deletion stimulates $O_2^{\cdot -}$ production (Fig. 4A). Anti-oxidant agents, either Tempol or Mito-Tempo treatment alleviated p16 elevation in AMPKα$2^{-/-}$ MEFs and consequent cellular senescence (Fig. 4B and 4D).These results suggest that AMPKα2 deletion upregulates p16 via reactive oxidative stress. On the other hand, p16 itself dampens intracellular ROS production independently of Rb pathway (Jenkins et al., 2011). P16 is upregulated in human melanocytes in response to H_2O_2-induced oxidative stress via a p38-mediated manner (Jenkins et al., 2011). We further presented evidence that transcription factor HBP1 is responsible for p16 induction in AMPKα$2^{-/-}$ MEFs. However, the regulation of HBP1 by oxidative stress warrants further extensive investigation. In addition, AMPK may regulate cell senescence through multiple pathways including autophagy (Kim et al., 2011).

Recently, it has been reported that AMPK activity is decreased with aging in human skin (Ido et al., 2015). However, there is no direct evidence to validate AMPK inhibition is the cause of skin aging. Here, we observed that AMPKα2 deletion in either young or old mice increases the number of senescent cells in the skin, while impeding the proliferative capacity evidenced by weaker staining of Ki-67. In addition, aged skin usually has reduced dermal thickness (Alexander et al., 2015; Branchet et al., 1990; Gambichler et al., 2006), whereas, AMPKα2-deleted mice have increased dermal thickness (Fig. 6). The cause and function of increased dermal thickness in AMPKα$2^{-/-}$ mice would be an important arena for future investigation.

In summary, our studies reveal an important role for AMPKα2 isoform in cell biology and connect two hallmarks of aging cells (Alexander et al., 2015; Lopez-Otin et al., 2013): cellular senescence and loss of proteostasis/proliferation capacity, which may be due to

HBP1 elevation. Given the importance of AMPK in cellular senescence, these findings hold profound implications for understanding the molecular mechanisms by which AMPK functions as a promising suppressor of cellular senescence, as well as tissue/organ aging.

Acknowledgements

This work was supported by funding from the following agencies: National Institutes of Health RO1 (HL110488, HL105157, HL096032, HL080499, HL089920, and HL079584) (all to M-H.Z.), Scientist Development Grant (11SDG5560036) from National Center of American Heart Association, Oklahoma Center for the Advancement of Science and Technology (OCAST) grant (HR12-061) (both to P.S.). M-H. Z. is a recipient of the National Established Investigator Award of the American Heart Association.

Abbreviations

AMPK	adenosine monophosphate-activated protein kinase
HBP1	HMG box-containing protein 1
HP1γ	heterochromatin protein 1 homolog gamma
ROS	reactive oxygen species

References

Alexander PB, Yuan L, Yang P, Sun T, Chen R, Xiang H, Chen J, Wu H, Radiloff DR, Wang XF. Egf promotes mammalian cell growth by suppressing cellular senescence. Cell Res. 2015; 25:135–138. [PubMed: 25367123]

Apfeld J, O'Connor G, McDonagh T, DiStefano PS, Curtis R. The amp-activated protein kinase aak-2 links energy levels and insulin-like signals to lifespan in c. Elegans. Genes Dev. 2004; 18:3004–3009. [PubMed: 15574588]

Baker DJ, Wijshake T, Tchkonia T, LeBrasseur NK, Childs BG, van de Sluis B, Kirkland JL, van Deursen JM. Clearance of p16ink4a-positive senescent cells delays ageing-associated disorders. Nature. 2011; 479:232–236. [PubMed: 22048312]

Braig M, Lee S, Loddenkemper C, Rudolph C, Peters AH, Schlegelberger B, Stein H, Dorken B, Jenuwein T, Schmitt CA. Oncogene-induced senescence as an initial barrier in lymphoma development. Nature. 2005; 436:660–665. [PubMed: 16079837]

Branchet MC, Boisnic S, Frances C, Robert AM. Skin thickness changes in normal aging skin. Gerontology. 1990; 36:28–35. [PubMed: 2384222]

Burd CE, Sorrentino JA, Clark KS, Darr DB, Krishnamurthy J, Deal AM, Bardeesy N, Castrillon DH, Beach DH, Sharpless NE. Monitoring tumorigenesis and senescence in vivo with a p16(ink4a)-luciferase model. Cell. 2013; 152:340–351. [PubMed: 23332765]

Chen D, Li PW, Goldstein BA, Cai W, Thomas EL, Chen F, Hubbard AE, Melov S, Kapahi P. Germline signaling mediates the synergistically prolonged longevity produced by double mutations in daf-2 and rsks-1 in c. Elegans. Cell reports. 2013; 5:1600–1610. [PubMed: 24332851]

Debacq-Chainiaux F, Erusalimsky JD, Campisi J, Toussaint O. Protocols to detect senescence-associated beta-galactosidase (sa-betagal) activity, a biomarker of senescent cells in culture and in vivo. Nat Protoc. 2009; 4:1798–1806. [PubMed: 20010931]

Fyhrquist F, Saijonmaa O, Strandberg T. The roles of senescence and telomere shortening in cardiovascular disease. Nature reviews Cardiology. 2013; 10:274–283. [PubMed: 23478256]

Gambichler T, Matip R, Moussa G, Altmeyer P, Hoffmann K. In vivo data of epidermal thickness evaluated by optical coherence tomography: Effects of age, gender, skin type, and anatomic site. J Dermatol Sci. 2006; 44:145–152. [PubMed: 17071059]

Ha L, Merlino G, Sviderskaya EV. Melanomagenesis: Overcoming the barrier of melanocyte senescence. Cell Cycle. 2008; 7:1944–1948. [PubMed: 18604170]

Hardie DG. Amp-activated/snf1 protein kinases: Conserved guardians of cellular energy. Nat Rev Mol Cell Biol. 2007; 8:774–785. [PubMed: 17712357]

Ido Y, Duranton A, Lan F, Weikel KA, Breton L, Ruderman NB. Resveratrol prevents oxidative stress-induced senescence and proliferative dysfunction by activating the ampk-foxo3 cascade in cultured primary human keratinocytes. PLoS One. 2015; 10:e0115341. [PubMed: 25647160]

Inwald EC, Klinkhammer-Schalke M, Hofstadter F, Zeman F, Koller M, Gerstenhauer M, Ortmann O. Ki-67 is a prognostic parameter in breast cancer patients: Results of a large population-based cohort of a cancer registry. Breast cancer research and treatment. 2013; 139:539–552. [PubMed: 23674192]

Janzen V, Forkert R, Fleming HE, Saito Y, Waring MT, Dombkowski DM, Cheng T, DePinho RA, Sharpless NE, Scadden DT. Stem-cell ageing modified by the cyclin-dependent kinase inhibitor p16ink4a. Nature. 2006; 443:421–426. [PubMed: 16957735]

Jenkins NC, Liu T, Cassidy P, Leachman SA, Boucher KM, Goodson AG, Samadashwily G, Grossman D. The p16(ink4a) tumor suppressor regulates cellular oxidative stress. Oncogene. 2011; 30:265–274. [PubMed: 20838381]

Jiao R, Postnikoff S, Harkness TA, Arnason TG. The snf1 kinase ubiquitin-associated domain restrains its activation, activity, and the yeast life span. J Biol Chem. 2015; 290:15393–15404. [PubMed: 25869125]

Jorgensen SB, Viollet B, Andreelli F, Frosig C, Birk JB, Schjerling P, Vaulont S, Richter EA, Wojtaszewski JF. Knockout of the alpha2 but not alpha1 5'-amp-activated protein kinase isoform abolishes 5-aminoimidazole-4-carboxamide-1-beta-4-ribofuranosidebut not contraction-induced glucose uptake in skeletal muscle. J Biol Chem. 2004; 279:1070–1079. [PubMed: 14573616]

Jung JK, Arora P, Pagano JS, Jang KL. Expression of DNA methyltransferase 1 is activated by hepatitis b virus × protein via a regulatory circuit involving the p16ink4a-cyclin d1-cdk 4/6-prb-e2f1 pathway. Cancer Res. 2007; 67:5771–5778. [PubMed: 17575144]

Kim J, Kundu M, Viollet B, Guan KL. Ampk and mtor regulate autophagy through direct phosphorylation of ulk1. Nat Cell Biol. 2011; 13:132–141. [PubMed: 21258367]

Kovacic JC, Moreno P, Hachinski V, Nabel EG, Fuster V. Cellular senescence, vascular disease, and aging: Part 1 of a 2-part review. Circulation. 2011; 123:1650–1660. [PubMed: 21502583]

Krishnamurthy J, Torrice C, Ramsey MR, Kovalev GI, Al-Regaiey K, Su L, Sharpless NE. Ink4a/arf expression is a biomarker of aging. J Clin Invest. 2004; 114:1299–1307. [PubMed: 15520862]

Lanna A, Henson SM, Escors D, Akbar AN. The kinase p38 activated by the metabolic regulator ampk and scaffold tab1 drives the senescence of human t cells. Nature immunology. 2014; 15:965–972. [PubMed: 25151490]

Li H, Wang W, Liu X, Paulson KE, Yee AS, Zhang X. Transcriptional factor hbp1 targets p16(ink4a), upregulating its expression and consequently is involved in ras-induced premature senescence. Oncogene. 2010; 29:5083–5094. [PubMed: 20581871]

Liang X, Wang P, Gao Q, Xiang T, Tao X. Endogenous lkb1 knockdown accelerates g(1)/s transition through p53 and p16 pathways. Cancer biology & therapy. 2010; 9:156–160. [PubMed: 20368693]

Lopez-Otin C, Blasco MA, Partridge L, Serrano M, Kroemer G. The hallmarks of aging. Cell. 2013; 153:1194–1217. [PubMed: 23746838]

Lu JY, Lin YY, Sheu JC, Wu JT, Lee FJ, Chen Y, Lin MI, Chiang FT, Tai TY, Berger SL, Zhao Y, Tsai KS, Zhu H, Chuang LM, Boeke JD. Acetylation of yeast ampk controls intrinsic aging independently of caloric restriction. Cell. 2011; 146:969–979. [PubMed: 21906795]

Meng S, Luo M, Sun H, Yu X, Shen M, Zhang Q, Zhou R, Ju X, Tao W, Liu D, Deng H, Lu Z. Identification and characterization of bmi-1-responding element within the human p16 promoter. J Biol Chem. 2010; 285:33219–33229. [PubMed: 20551323]

Munoz-Espin D, Serrano M. Cellular senescence: From physiology to pathology. Nat Rev Mol Cell Biol. 2014; 15:482–496. [PubMed: 24954210]

O'Donnell KA, Wentzel EA, Zeller KI, Dang CV, Mendell JT. C-myc-regulated microrna modulate e2f1 expression. Nature. 2005; 435:839–843. [PubMed: 15944709]

Ohtani N, Zebedee Z, Huot TJ, Stinson JA, Sugimoto M, Ohashi Y, Sharrocks AD, Peters G, Hara E. Opposing effects of ets and id proteins on p16ink4a expression during cellular senescence. Nature. 2001; 409:1067–1070. [PubMed: 11234019]

Rayess H, Wang MB, Srivatsan ES. Cellular senescence and tumor suppressor gene p16. Int J Cancer. 2012; 130:1715–1725. [PubMed: 22025288]

Reznick RM, Zong H, Li J, Morino K, Moore IK, Yu HJ, Liu ZX, Dong J, Mustard KJ, Hawley SA, Befroy D, Pypaert M, Hardie DG, Young LH, Shulman GI. Aging-associated reductions in amp-activated protein kinase activity and mitochondrial biogenesis. Cell Metab. 2007; 5:151–156. [PubMed: 17276357]

Ruderman NB, Carling D, Prentki M, Cacicedo JM. Ampk, insulin resistance, and the metabolic syndrome. J Clin Invest. 2013; 123:2764–2772. [PubMed: 23863634]

Rufini A, Tucci P, Celardo I, Melino G. Senescence and aging: The critical roles of p53. Oncogene. 2013; 32:5129–5143. [PubMed: 23416979]

Salminen A, Kaarniranta K. Amp-activated protein kinase (ampk) controls the aging process via an integrated signaling network. Ageing research reviews. 2012; 11:230–241. [PubMed: 22186033]

Song P, Wang S, He C, Liang B, Viollet B, Zou MH. Ampkalpha2 deletion exacerbates neointima formation by upregulating skp2 in vascular smooth muscle cells. Circ Res. 2011; 109:1230–1239. [PubMed: 21980125]

Song P, Wu Y, Xu J, Xie Z, Dong Y, Zhang M, Zou MH. Reactive nitrogen species induced by hyperglycemia suppresses akt signaling and triggers apoptosis by upregulating phosphatase pten (phosphatase and tensin homologue deleted on chromosome 10) in an lkb1-dependent manner. Circulation. 2007; 116:1585–1595. [PubMed: 17875968]

Song P, Zhang M, Wang S, Xu J, Choi HC, Zou MH. Thromboxane a2 receptor activates a rho-associated kinase/lkb1/pten pathway to attenuate endothelium insulin signaling. J Biol Chem. 2009; 284:17120–17128. [PubMed: 19403525]

Song P, Zou MH. Regulation of nad(p)h oxidases by ampk in cardiovascular systems. Free Radic Biol Med. 2012; 52:1607–1619. [PubMed: 22357101]

Sorrentino JA, Krishnamurthy J, Tilley S, Alb JG Jr, Burd CE, Sharpless NE. P16ink4a reporter mice reveal age-promoting effects of environmental toxicants. J Clin Invest. 2014; 124:169–173. [PubMed: 24334456]

Stenesen D, Suh JM, Seo J, Yu K, Lee KS, Kim JS, Min KJ, Graff JM. Adenosine nucleotide biosynthesis and ampk regulate adult life span and mediate the longevity benefit of caloric restriction in flies. Cell Metab. 2013; 17:101–112. [PubMed: 23312286]

Sung JY, Woo CH, Kang YJ, Lee KY, Choi HC. Ampk induces vascular smooth muscle cell senescence via lkb1 dependent pathway. Biochem Biophys Res Commun. 2011; 413:143–148. [PubMed: 21872575]

Testa R, Ceriello A. Pathogenetic loop between diabetes and cell senescence. Diabetes Care. 2007; 30:2974–2975. [PubMed: 17965314]

Todaro GJ, Green H. Quantitative studies of the growth of mouse embryo cells in culture and their development into established lines. J Cell Biol. 1963; 17:299–313. [PubMed: 13985244]

Tsuchihashi NA, Hayashi K, Dan K, Goto F, Nomura Y, Fujioka M, Kanzaki S, Komune S, Ogawa K. Autophagy through 4ebp1 and ampk regulates oxidative stress-induced premature senescence in auditory cells. Oncotarget. 2015; 6:3644–3655. [PubMed: 25682865]

van Deursen JM. The role of senescent cells in ageing. Nature. 2014; 509:439–446. [PubMed: 24848057]

Viollet B, Andreelli F, Jorgensen SB, Perrin C, Geloen A, Flamez D, Mu J, Lenzner C, Baud O, Bennoun M, Gomas E, Nicolas G, Wojtaszewski JF, Kahn A, Carling D, Schuit FC, Birnbaum MJ, Richter EA, Burcelin R, Vaulont S. The amp-activated protein kinase alpha2 catalytic subunit controls whole-body insulin sensitivity. J Clin Invest. 2003; 111:91–98. [PubMed: 12511592]

Waaijer ME, Parish WE, Strongitharm BH, van Heemst D, Slagboom PE, de Craen AJ, Sedivy JM, Westendorp RG, Gunn DA, Maier AB. The number of p16ink4a positive cells in human skin reflects biological age. Aging cell. 2012; 11:722–725. [PubMed: 22612594]

Wang S, Song P, Zou MH. Inhibition of amp-activated protein kinase alpha (ampkalpha) by doxorubicin accentuates genotoxic stress and cell death in mouse embryonic fibroblasts and cardiomyocytes: Role of p53 and sirt1. J Biol Chem. 2012a; 287:8001–8012. [PubMed: 22267730]

Wang S, Zhang M, Liang B, Xu J, Xie Z, Liu C, Viollet B, Yan D, Zou MH. Ampkalpha2 deletion causes aberrant expression and activation of nad(p)h oxidase and consequent endothelial

dysfunction in vivo: Role of 26s proteasomes. Circ Res. 2010; 106:1117–1128. [PubMed: 20167927]

Wang W, Pan K, Chen Y, Huang C, Zhang X. The acetylation of transcription factor hbp1 by p300/cbp enhances p16ink4a expression. Nucleic acids research. 2012b; 40:981–995. [PubMed: 21967847]

Wang W, Yang X, Lopez de Silanes I, Carling D, Gorospe M. Increased amp:Atp ratio and amp-activated protein kinase activity during cellular senescence linked to reduced hur function. J Biol Chem. 2003; 278:27016–27023. [PubMed: 12730239]

Xia W, Zhang F, Xie C, Jiang M, Hou M. Macrophage migration inhibitory factor confers resistance to senescence through cd74-dependent ampk-foxo3a signaling in mesenchymal stem cells. Stem Cell Res Ther. 2015; 6:82. [PubMed: 25896286]

Xu H, Zhou Y, Coughlan KA, Ding Y, Wang S, Wu Y, Song P, Zou MH. Ampkalpha1 deficiency promotes cellular proliferation and DNA damage via p21 reduction in mouse embryonic fibroblasts. Biochim Biophys Acta. 2015; 1853:65–73. [PubMed: 25307521]

Yi G, He Z, Zhou X, Xian L, Yuan T, Jia X, Hong J, He L, Liu J. Low concentration of metformin induces a p53-dependent senescence in hepatoma cells via activation of the ampk pathway. Int J Oncol. 2013; 43:1503–1510. [PubMed: 23982736]

Zheng Y, He L, Wan Y, Song J. H3k9me-enhanced DNA hypermethylation of the p16ink4a gene: An epigenetic signature for spontaneous transformation of rat mesenchymal stem cells. Stem cells and development. 2013; 22:256–267. [PubMed: 22873822]

Highlights

- AMPKα2 deletion leads to cellular senescence
- Deletion of AMPKα2 is associated with an induction in p16
- Antioxidant partially decreases p16 and subsequent cell senescence
- Knockdown of HMG box-containing protein 1 (HBP1) blocks the cellular senescence via p16 reduction

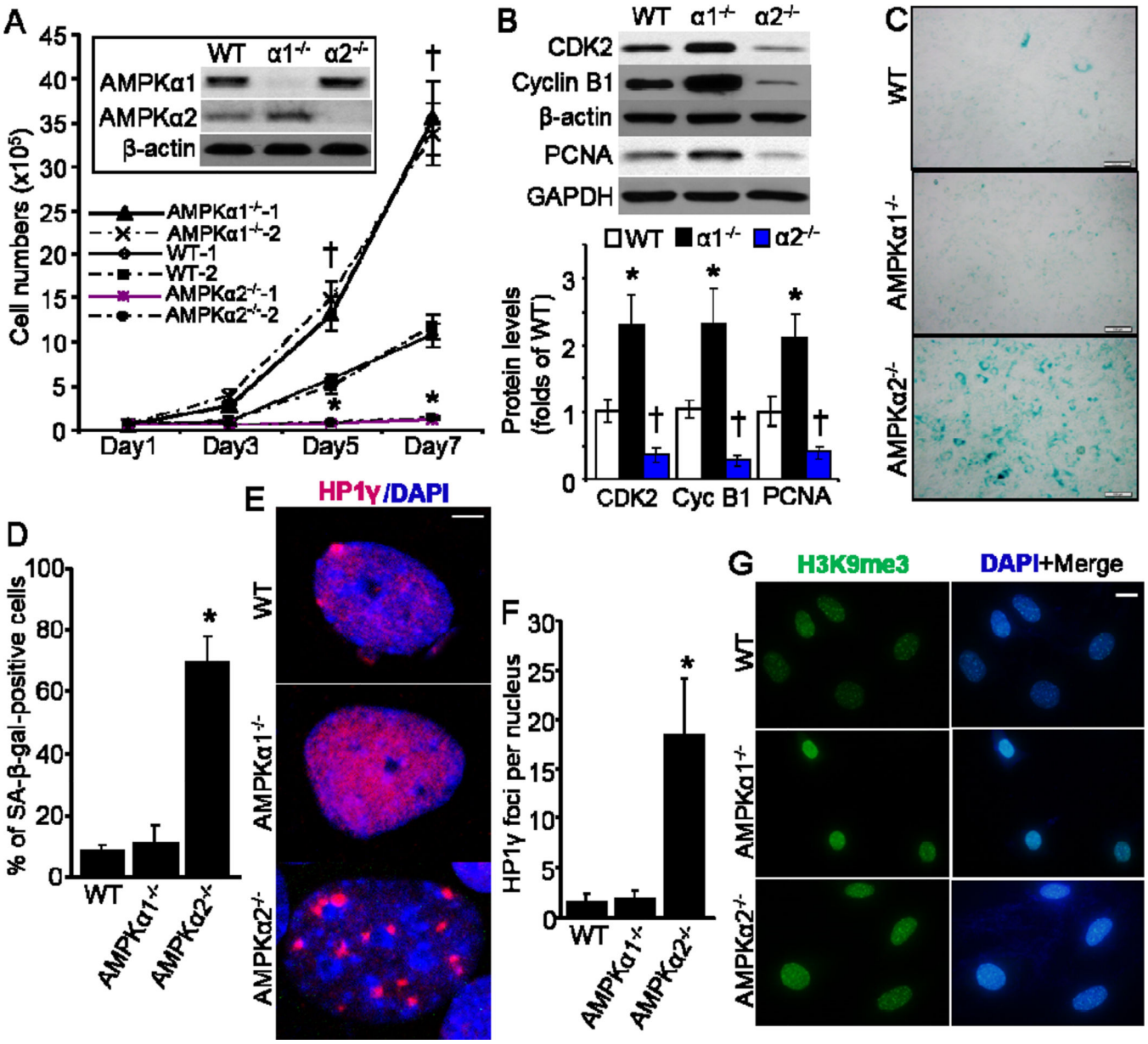

Fig. 1.

Deficiency of AMPKα2, but not AMPKα1, leads to enhanced cellular senescence in MEFs. (A) Wild type (WT), AMPKα1$^{-/-}$ and AMPKα2$^{-/-}$ MEFs (two independent cell lines for each) were seeded with 0.5 × 10^5 cells in 6-well plates. Cell number counting was taken at different time point. n=8, *p< 0.05 vs WT, †p< 0.01 vs WT. Representative Western blot of AMPKα1 and AMPKα2 was shown as an inset of bar graph. (B) Profile of cellular proliferation-associated proteins, including CDK2, Cyclin B1, and PCNA. n=6, *p< 0.01 vs WT, †p< 0.01 vs WT. (C) Representative images showing SA-β-galactosidase (SA-β-gal) activity in WT, AMPKα1$^{-/-}$, and AMPKα2$^{-/-}$ MEFs. Scale bar = 50 μm. (D) Percentage of SA-β-gal-positive cells in cultured MEFs. n=10, *p< 0.05 vs WT. (E) HP1γ foci formation was increased in AMPKα2$^{-/-}$ MEFs. Representative images showing HP1γ foci formation (red color), marking senescence. Scale bar = 2.5 μm. (F) Quantitative analysis of HP1γ foci

per nucleus. n=20, *p< 0.01 vs WT. (G) Representative images showing staining of anti-H3k9me3. Scale bar = 20 μm.

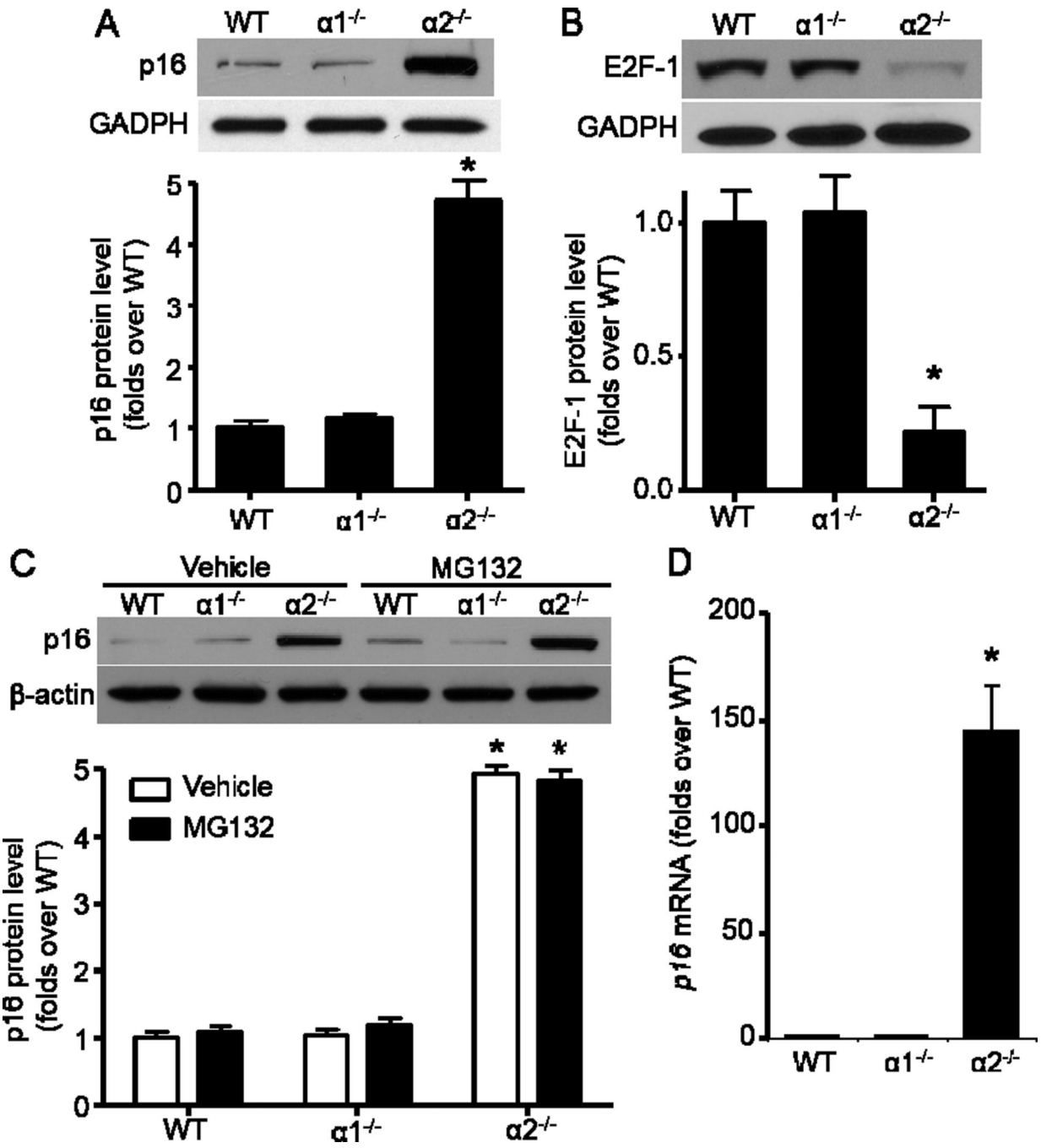

Fig. 2.

Transcriptional upregulation of p16 in AMPKα2$^{-/-}$ MEFs. (A) (Upper) AMPKα2 deletion significantly upregulated p16. (Bottom) Quantification of Western blot data. n=8, *p< 0.001 vs WT. (B) (Upper) AMPKα2 deletion significantly down-regulated E2F1. (Bottom) Quantification of Western blot data. n=6, *p< 0.001 vs WT. (C) Proteasome inhibitor, MG132 (20 μM, 8 h) did not further increase p16 in AMPKα2$^{-/-}$ MEFs. n=4, *p< 0.001 vs WT. (D) Quantitative RT-PCR analysis of p16 expression in MEFs. β-actin was used as

endogenous loading control. Values are mean ± SEM of four independent experiments, *p< 0.001 vs WT.

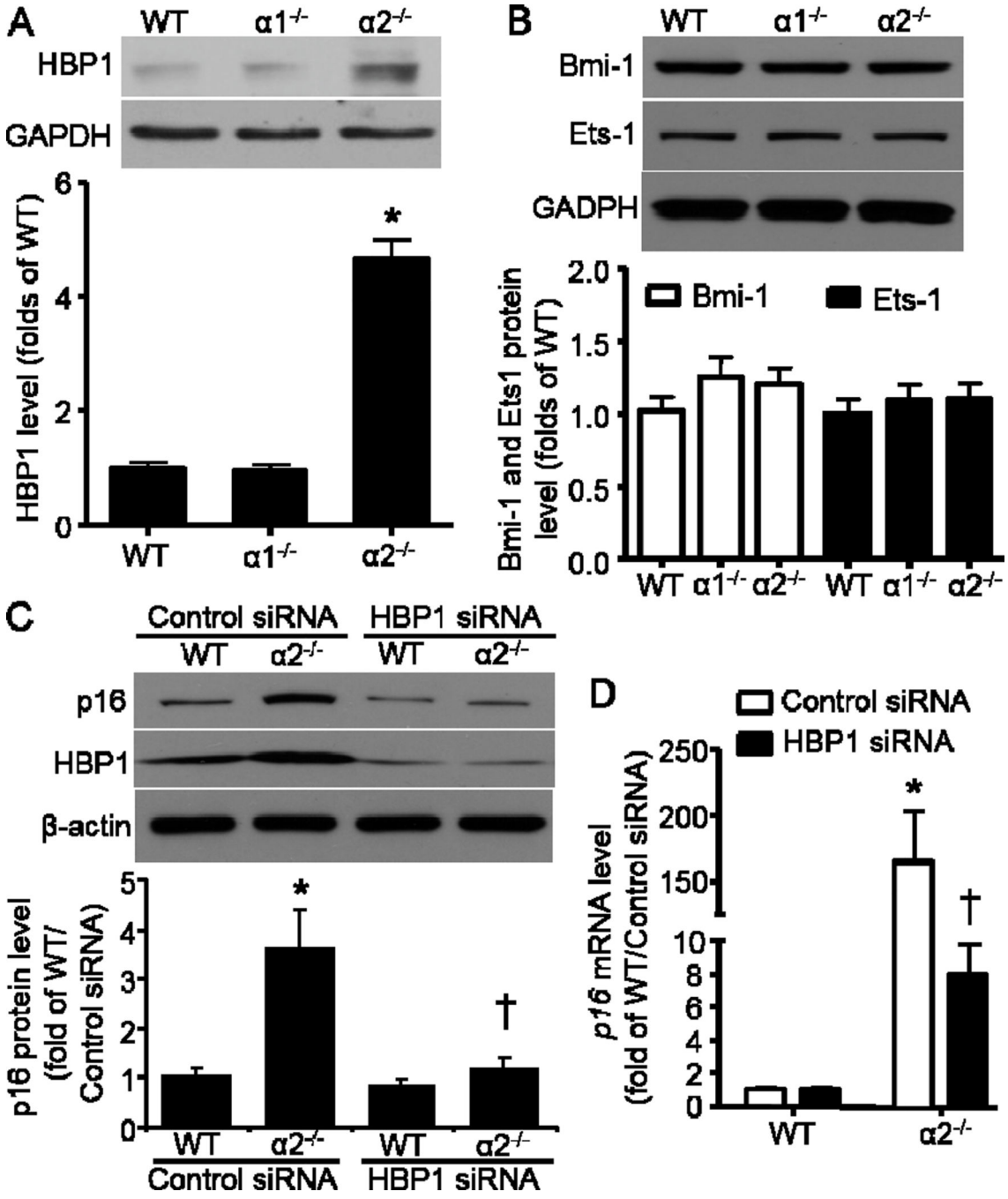

Fig. 3.

HBP1 is responsible for p16 induction in AMPKa2$^{-/-}$ MEFs. (A) (Upper) AMPKα2 deletion significantly upregulated HBP1. (Bottom) Quantification of Western blot data. n=6, *p< 0.001 vs WT. (B) Neither AMPKa2 nor AMPKa1 deletion altered Bmi-1 and Ets1 protein levels. (C) (Upper) HBP1 knockdown by siRNA reversed p16 elevation in AMPKa2$^{-/-}$ MEFs. (Bottom) Quantification of Western blot data. n=4, *p< 0.01 vs WT/ Control siRNA, †p< 0.01 vs a2$^{-/-}$/Control siRNA. (D) HBP1 siRNA significantly

downregulated p16 mRNA level in AMPKa2$^{-/-}$ MEFs. n=6, *p< 0.01 vs WT/Control siRNA, †p< 0.01 vs a2$^{-/-}$/Control siRNA.

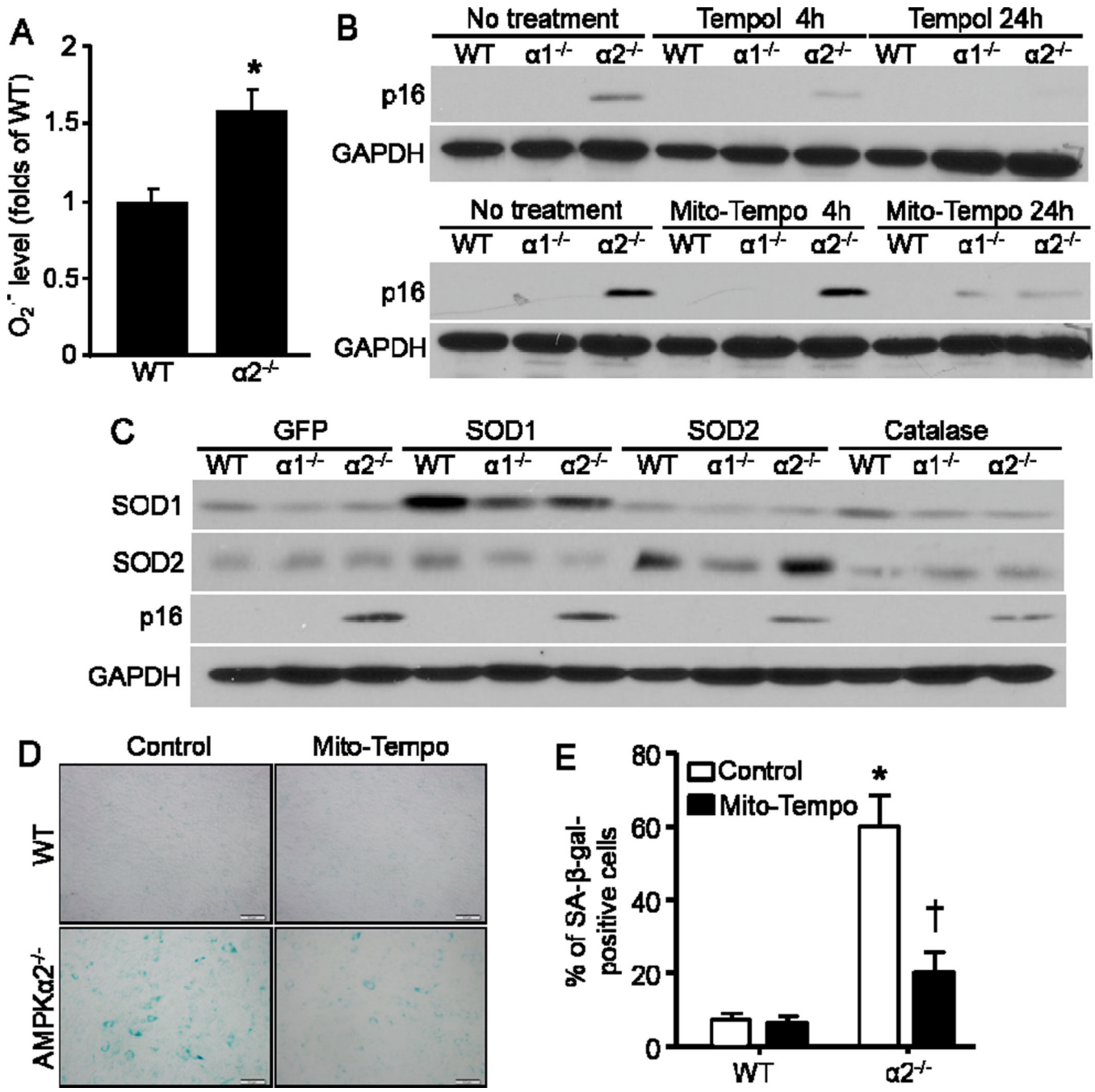

Fig. 4.

Increased ROS in AMPKα2$^{-/-}$ MEFs contributes to p16 upregulation. (A) AMPKα2 deletion elevated superoxide anion ($O^{2\,\bullet-}$) production. n=10, *p< 0.05 vs WT. (B) Anti-oxidants Tempol and Mito-Tempo inhibited p16 elevation in AMPKα2$^{-/-}$ MEFs. (C) SOD2 and Catalase dampened p16 induction in AMPKα2$^{-/-}$ MEFs. (D) Representative images indicated that Mito-Tempo blunted cellular senescence of AMPKα2$^{-/-}$ MEFs demonstrated by SA-β-gal staining. (E) Percentage of SA-β-gal-positive cells in Mito-Tempo-treated MEFs. n=10, *p< 0.001 vs WT/Control, †p< 0.01 vs a2$^{-/-}$/Control. Scale bar = 50 μm.

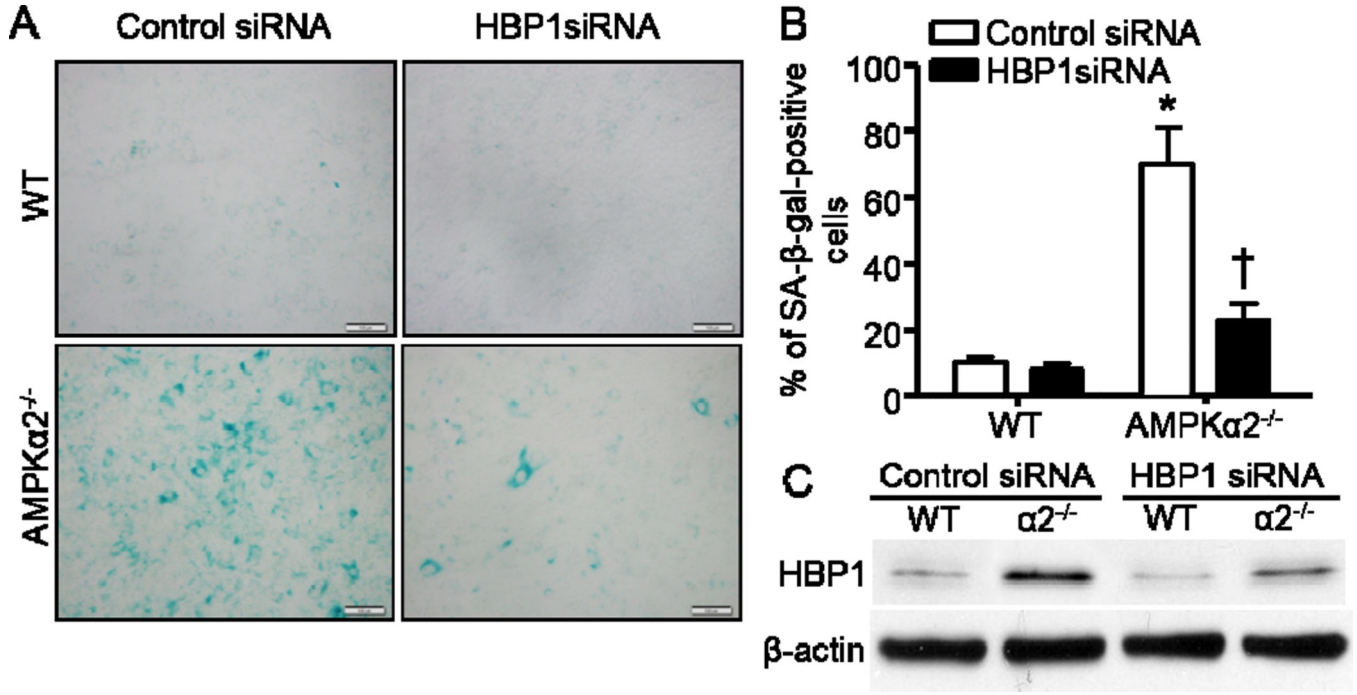

Fig. 5.

HBP1 is responsible for the cellular senescence in AMPKα2$^{-/-}$ MEFs. (A) Representative images indicated that HBP1 knockdown by siRNA blunted cell senescence in AMPKα2$^{-/-}$ MEFs. Scale bar = 50 μm. (B) Quantification of SA-β-gal staining. n=6, *p< 0.001 vs WT/Control siRNA, †p< 0.01 vs AMPKa2$^{-/-}$/Control siRNA. (C) Representative Western blot of HBP1.

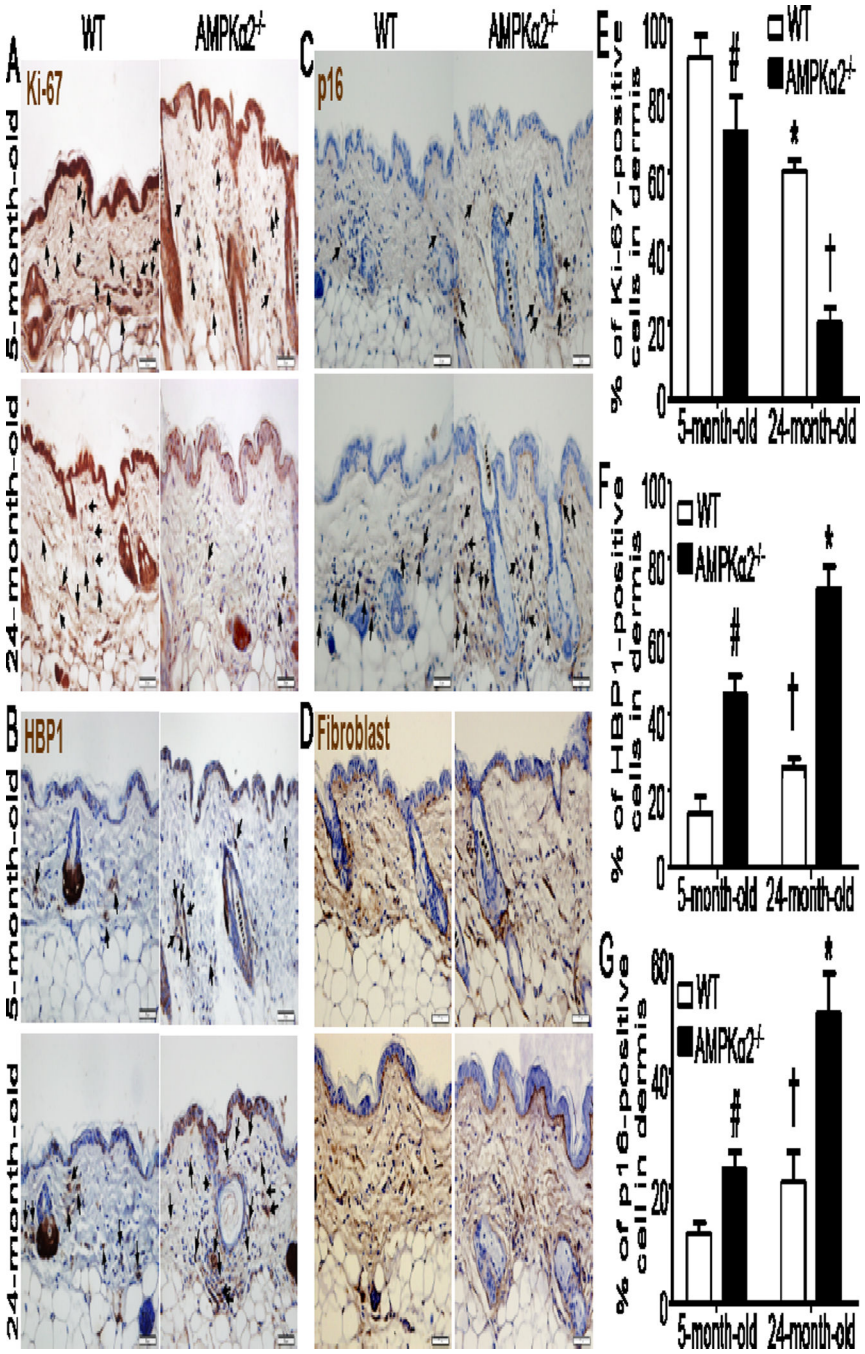

Fig. 6.

Increased senescent cells in the skin of AMPKα2$^{-/-}$ mice compared with wild type (WT) mice. (A) Ki-67 staining (brown) was decreased in the skin of 24-month-old AMPKα2$^{-/-}$ mice. (B) HBP1 (brown color) was increased in derma fibroblast and skin of 24-month-old AMPKα2$^{-/-}$ mice. (C) p16 (brown staining) was increased in derma fibroblast and skin of 24-month-old AMPKα2$^{-/-}$ mice. (D) Staining of fibroblast marker in skin of young and old wild WT and AMPKα2$^{-/-}$ mice. All sections were counterstained with hematoxylin to detect nuclei (blue color). Arrows indicate the brown-stained cells. Scale bar = 50 μm. (E)

Quantification of Ki-67-positive cells in dermis. n=10 in each group, # $p<0.05$ vs WT/5-month-old, * $p<0.01$ vs WT/5-month-old, †$p<0.001$ vs WT/24-month-old. (F) Quantification of HBP1-positive cells in dermis. n=10, # $p<0.01$ vs WT/5-month-old, † $p<0.05$ vs WT/5-month-old, * $p<0.01$ vs WT/24-month-old. (G) Quantification of p16-positive cells in dermis. n=10, # $p<0.01$ vs WT/5-month-old, † $p<0.05$ vs WT/5-month-old, *$p<0.01$ vs WT/24-month-old.

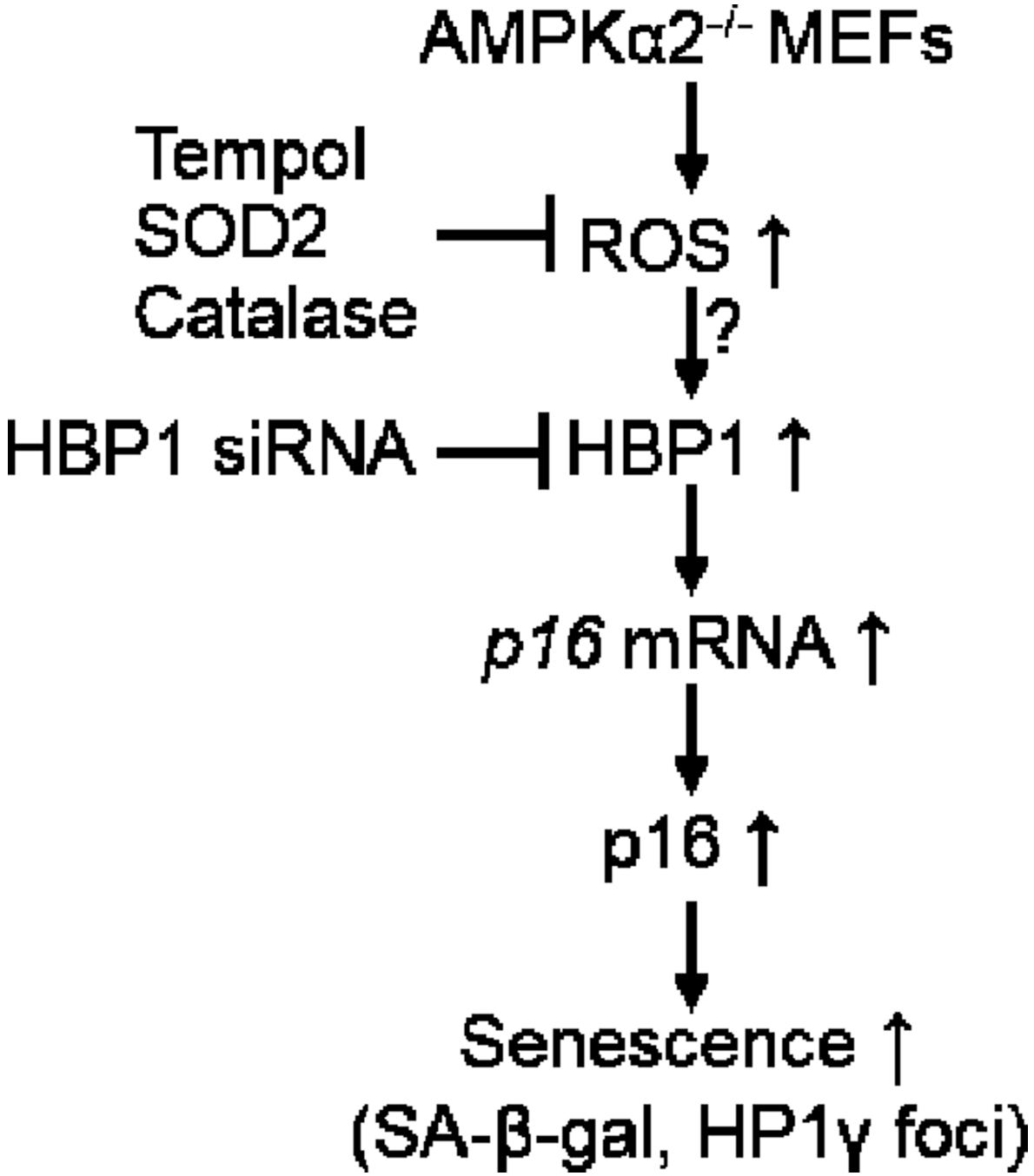

Fig. 7.

Proposed mechanism underlying AMPKα2 deletion-stimulated cellular senescence. Absence of AMPKα2 will increase ROS production, which leads to p16 upregulation mediated by HBP1.